

Reactivity of a (Benzene)Ruthenium(II) Cation on Di-lacunary γ -Keggin-Type Silicotungstate and Synthesis of a Mono-(Benzene)Ruthenium(II)-Attached γ -Keggin-Type Silicotungstate

Masaya Kikuchi,^[a] Hiromi Ota,^[b] Xavier López,^[c] Toshimi Nakaya,^{[a][d]} Nao Tsunoji,^[a] Tsuneji Sano,^[a] and Masahiro Sadakane*^[a]

Abstract: Reaction of a (benzene)Ru²⁺ complex, [Ru(C₆H₆)Cl₂]₂, with a di-lacunary γ -Keggin-type silicotungstate, K₈[γ -SiW₁₀O₃₆], at a (C₆H₆)Ru²⁺/[γ -SiW₁₀O₃₆]⁸⁻ ratio of 1 produces [γ -SiW₁₀O₃₆Ru(C₆H₆)]⁶⁻. The cesium salt was characterized using experimental and theoretical methods; one (C₆H₆)Ru²⁺ moiety is attached through three bridging oxygens of the non-lacunary site, and the anion is stable in aqueous solution. ¹H NMR and high-resolution electrospray ionization mass spectrometry measurements of the reaction mixture with different (C₆H₆)Ru²⁺/[γ -SiW₁₀O₃₆]⁸⁻ ratios indicate that the (C₆H₆)Ru²⁺ complex first reacts with the three bridging oxygens of the non-lacunary site to form [γ -SiW₁₀O₃₆Ru(C₆H₆)]⁶⁻, and then react on the terminal oxygens of the lacunary site to form a [γ -SiW₁₀O₃₆Ru(C₆H₆)]⁴⁻ complex, which was reported by the Kortz and Nadjo group (Bi et al., *Inorg. Chem.* **2006**, *45*, 8575-8583).

Introduction

Heteropolytungstates are anionic mixed tungsten oxide molecules that have attracted increasing interest because of their redox activities, photochemical properties, and acidic properties; they have been utilized as catalysts and functional materials.^[1] Among them, considerable attention has been directed toward a di-lacunary γ -Keggin-type silicotungstate, [γ -SiW₁₀O₃₆]⁸⁻, where

two tungsten atoms are removed from the parent Keggin-type silicotungstate, [SiW₁₂O₄₀]⁴⁻. Mizuno's group extensively investigated the reactivity and catalytic activity of [γ -SiW₁₀O₃₆]⁸⁻ and identified several interesting properties.^[2] The di-lacunary γ -Keggin-type silicotungstate shows a high catalytic activity for oxidation of olefins, allylic alcohols, sulfides, and silanes using H₂O₂ as an oxidant,^[2] and its catalytic activity depends on the number of protons that attach to the molecule.^[2b, 2d, 3] Furthermore, [γ -SiW₁₀O₃₆]⁸⁻ shows interesting photocatalytic activities in the presence of alcohols.^[4] Protons can attach to the terminal oxygens of the lacunary site and to the bridging oxygens of the non-lacunary site (Figure 1a, white arrows).^[5] Another important property is that the anion can incorporate other elements on the lacunary site to form multi-metal-containing silicotungstates and show a variety of catalytic activities^[2a, 2c, 6] and magnetic properties.^[7] One of the most important examples is a tetra-Ru-containing sandwiched molecule, [(γ -SiW₁₀O₃₆)₂{Ru₄O₄(OH)₄(H₂O)₄}]¹⁰⁻, which is the most active water oxidation catalyst.^[8] It is therefore important to understand the reactivity of cationic species on [γ -SiW₁₀O₃₆]⁸⁻.

Ru-containing heteropolytungstates are some of the most important compounds in heteropolytungstate chemistry because the Ru atom shows unique redox properties, catalytic properties, and reactivities with organic compounds.^[9] The (arene)Ru²⁺ complex is one of the most investigated types of Ru species for modifying heteropolytungstates where Ru is coordinated by arene through η^3 -coordination and three coordination sites are available. The (arene)Ru²⁺ complex can bind to either three oxygens on the triangular face or two terminal oxygens of the lacunary heteropolytungstates. The (arene)Ru²⁺ complex can also bind to anionic molecular oxides of molybdenum, niobium, and tantalum.^[10]

The Kortz and Nadjo group reported that (C₆H₆)Ru²⁺ binds both to the terminal oxygen of the lacunary site and to three bridging oxygens on the non-lacunary position of [γ -SiW₁₀O₃₆]⁸⁻ to form a di-(C₆H₆)Ru-modified compound, [γ -SiW₁₀O₃₆Ru(C₆H₆)₂{Ru(C₆H₆)(H₂O)}]⁴⁻ (Figure 1c).^[11] This is a rare example whereby a metal binds to the bridging oxygens at the non-lacunary site, although protonation of the bridging oxygen on the non-lacunary site has been reported.^[5] Additionally, (C₆H₆)Ru²⁺ can both bind to the three oxygens of the lacunary site and those of the non-lacunary site of tri-lacunary silicotungstate, [SiW₉O₃₄]¹⁰⁻, to form [SiW₉O₃₄{Ru(C₆H₆)₂}]⁶⁻.^[12] Thus, it is important to understand the reactivity of the (arene)Ru²⁺ on heteropolytungstates because

[a] M. Kikuchi, T. Nakaya, N. Tsunoji, T. Sano, M. Sadakane
Department of Applied Chemistry, Graduate School of Engineering
Hiroshima University
1-4-1 Kagamiyama, Higashi-Hiroshima 739-8527, Japan
E-mail: sadakane09@hiroshima-u.ac.jp

[b] H. Ota
Division of Instrumental Analysis, Department of Instrumental
Analysis and Cryogenics Department, Advanced Science Research
Center
Okayama University
Okayama 700-8530, Japan

[c] X. López
Departament de Química Física i Inorgànica
Universitat Rovira i Virgili
Marcel·lí Domingo 1, 43007 Tarragona, Spain

[d] T. Nakaya
Technical Center
Hiroshima University
1-4-1 Kagamiyama, Higashi-Hiroshima 739-8527, Japan

Supporting information for this article is given via a link at the end of the document.

(arene)Ru²⁺-decorated heteropolytungstates show catalytic activity.^[13]

In this manuscript, we present (C₆H₆)Ru²⁺ first bound to the three bridging oxygens of the non-lacunary site to form [γ-SiW₁₀O₃₆Ru(C₆H₆)]⁶⁻.

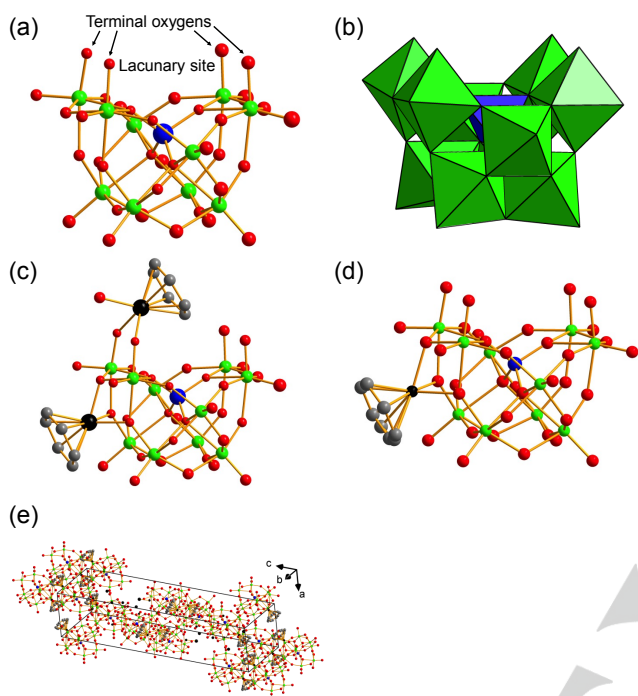


Figure 1. (a) Ball-and-stick and (b) polyhedral presentations of the di-lacunary γ -Keggin silicotungstate, [γ-SiW₁₀O₃₆]⁸⁻. Ball-and-stick presentation of (c) di-(C₆H₆)Ru-attached [γ-SiW₁₀O₃₆]⁸⁻, [γ-SiW₁₀O₃₆Ru(C₆H₆)(Ru(C₆H₆)(H₂O))]⁴⁺, and (d) mono-(C₆H₆)Ru attached [γ-SiW₁₀O₃₆]⁸⁻, [γ-SiW₁₀O₃₆Ru(C₆H₆)]⁶⁻. (e) Packing of [γ-SiW₁₀O₃₆Ru(C₆H₆)]⁶⁻ in a unit cell. Green, blue, black, red, grey, and black balls represent W, Si, Ru, O, C, and Cs, respectively.

Results and Discussion

Isolation and Structural Characterization

Mixing [Ru(C₆H₆)Cl₂]₂ and K₈[γ-SiW₁₀O₃₆] at a (C₆H₆)Ru²⁺/[γ-SiW₁₀O₃₆]⁸⁻ ratio of 1.0 at room temperature immediately produces an orange solution; adding CsCl to the reaction mixture produces orange solids. Recrystallization in water via vapor diffusion of ethanol produces orange crystals.

Single-crystal structure analysis reveals that the orange crystal contains di-lacunary γ -Keggin-type silicotungstate, [γ-SiW₁₀O₃₆]⁸⁻, with one (C₆H₆)Ru moiety attached through three Ru-O bonds to the bridging oxygens of the non-lacunary site to form the [γ-SiW₁₀O₃₆Ru(C₆H₆)]⁶⁻ molecule with C_s symmetry (Figure 1d). The polyanions are packed in a monoclinic crystal system with a Cs⁺ cation and water molecule (Figure 1d).

The IR spectrum of the isolated solid (Figure 2a) is similar to that of K₈[γ-SiW₁₀O₃₆] (Figure 2b) with slight band shifts that indicate the presence of the [γ-SiW₁₀O₃₆]⁸⁻ structure.

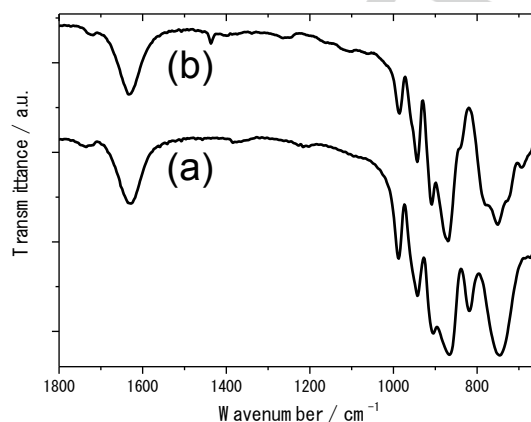


Figure 2. IR spectrum of (a) K₈[γ-SiW₁₀O₃₆] and (b) the isolated solid, Cs₆[γ-SiW₁₀O₃₆Ru(C₆H₆)].

¹H and ¹³C NMR spectra of the isolated orange solid dissolved in D₂O show singlets at 5.99 and 81.61 ppm, respectively (Figure 3a, d, e), indicating that the valence of Ru is 2+ and the isolated compound is pure. Solid-state ¹³C magic angle spinning (MAS) NMR of the solid shows one singlet at 83.05 ppm (Figure 3c), which is similar to the ¹³C NMR spectrum of the orange solid dissolved in D₂O, indicating that the structure is stable in water.

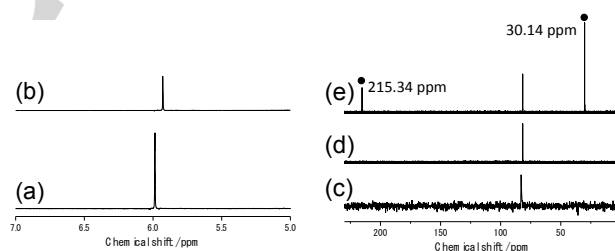


Figure 3. (Top) ¹H NMR of [γ-SiW₁₀O₃₆Ru(C₆H₆)]⁶⁻ dissolved in (a) D₂O and (b) acetate buffer in D₂O (pH 4.7). (Bottom) (c) ¹³C MAS NMR of Cs₆[γ-SiW₁₀O₃₆Ru(C₆H₆)], and ¹³C NMR of [γ-SiW₁₀O₃₆Ru(C₆H₆)]⁶⁻ dissolved in (d) D₂O and (e) D₂O with acetone as an internal standard.

¹⁸³W NMR of [γ-SiW₁₀O₃₆Ru(C₆H₆)]⁶⁻ dissolved in D₂O shows five singlets at -25.88, -50.06, -140.10, -150.85, and -187.17 ppm with the expected 1:1:1:1:1 integration ratio (Figure 4) for the [γ-SiW₁₀O₃₆Ru(C₆H₆)]⁶⁻ molecule with C_s symmetry. Two singlets are shifted downfield because the di-lacunary silicodetungstate [γ-SiW₁₀O₃₆]⁸⁻ with C_{2v} symmetry shows three singlets at -96.4, -137.2, and -158.2 ppm with a 2:2:1 integration ratio.^[14]

Two ¹⁸³W NMR peaks of W close to Ru in a mono-Ru²⁺-substituted heteropolytungstate, [PW₁₁O₃₉Ru(H₂O)]⁵⁻, show

downfield shifts (292 and 159 ppm).^[15] The degree of the downfield shift depends on the heteroatom and the ligand coordinated to Ru; the two most downfield-shifted W peaks of $[\text{PW}_{11}\text{O}_{39}\text{Ru}(\text{DMSO})]^{5-}$ (DMSO = dimethyl sulfoxide) are observed at 118 and -2 ppm^[15-16] and those of $[\text{SiW}_{11}\text{O}_{39}\text{Ru}(\text{CO})]^{6-}$ are observed at 72 and -70 ppm.^[17] For (arene) Ru^{2+} -containing heteropolytungstates, such as $[\text{PW}_{11}\text{O}_{39}\{\text{Ru}(\textit{p}\text{-cymene})(\text{H}_2\text{O})\}]^{5-}$, $[\text{PW}_{11}\text{O}_{39}\{\text{Ru}(\textit{p}\text{-cymene})\}_2(\text{WO}_2)]^{5-}$, and $[\text{Sb}_2\text{W}_{20}\text{O}_{40}\{\text{Ru}(\textit{p}\text{-cymene})\}_2]^{10-}$, all ^{183}W NMR peaks appear at positions more negative than -70 ppm.^[18] For the di-(C_6H_6)Ru-containing tri-lacunary heteropolytungstates, $[\text{SiW}_9\text{O}_{34}\{\text{Ru}(\text{C}_6\text{H}_6)\}_2]^{6-}$ and $[\text{GeW}_9\text{O}_{34}\{\text{Ru}(\text{C}_6\text{H}_6)\}_2]^{6-}$, only one ^{183}W NMR peak appears with a large downfield shift (at ~ 53 ppm and ~ 25 ppm, respectively) and other peaks appear more negative than -90 ppm, although three kinds of W atoms bind to the (C_6H_6)Ru moiety through Ru-O-W bonds.^[12] For $[\text{X}_2\text{W}_{20}\text{O}_{40}\{\text{Ru}(\text{C}_6\text{H}_6)\}_2]^{10-}$ ($\text{X} = \text{Sb}$ or Bi), where two W atoms are close to the Ru center, the most downfield-shifted peak appears at approximately -60 or -30 ppm, depending on the heteroatom, and others appear more negative than -80 ppm.^[13] These results indicate that the chemical shifts of W connected to the Ru^{2+} moiety through an oxygen appear in a wide range between 120 and -120 ppm, and the most downfield-shifted peaks at -25.88 and -50.06 ppm may be assignable to W close to Ru. The structure obtained from single-crystal X-ray diffraction (XRD) shows two kinds of W atoms close to Ru, and the structure is stable in aqueous solution.

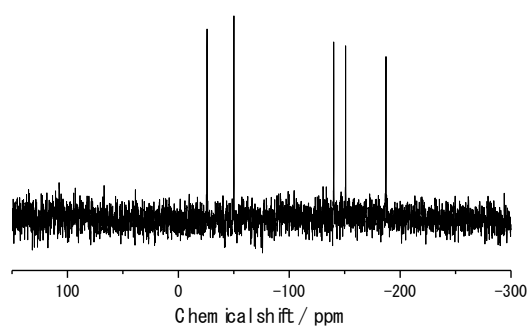
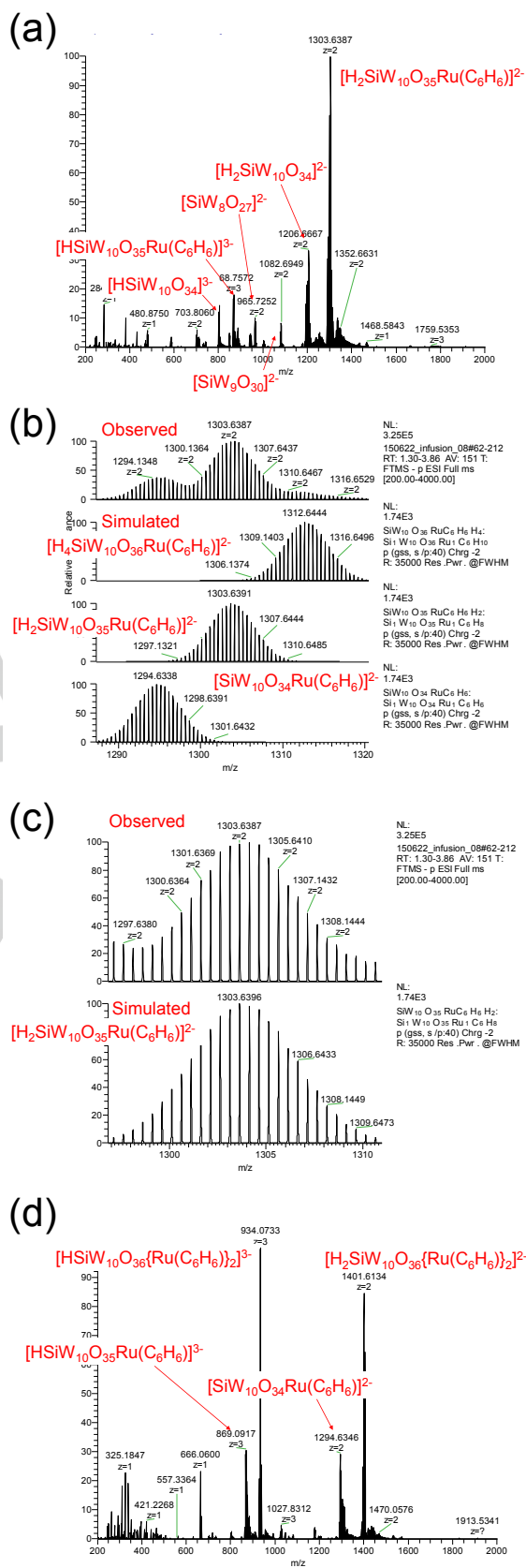


Figure 4. ^{183}W NMR of $[\gamma\text{-SiW}_{10}\text{O}_{36}\text{Ru}(\text{C}_6\text{H}_6)]^{5-}$ dissolved in D_2O with the help of a Li resin.

The most intense signal in the high-resolution electrospray ionization (HR-ESI) mass spectrum (MS) of isolated $[\gamma\text{-SiW}_{10}\text{O}_{36}\text{Ru}(\text{C}_6\text{H}_6)]^{6-}$ is assignable to $\text{H}_2[\text{SiW}_{10}\text{O}_{35}\text{Ru}(\text{C}_6\text{H}_6)]^{2-}$, which is a mono-dehydrated species of $\text{H}_4[\text{SiW}_{10}\text{O}_{36}\text{Ru}(\text{C}_6\text{H}_6)]^{2-}$ (Figure 5). Elemental analysis of the isolated orange solid reveals that the formula is $\text{Cs}_6[\text{SiW}_{10}\text{O}_{36}\text{Ru}(\text{C}_6\text{H}_6)]$. These results indicate that the isolated orange solid is a cesium salt of a 1:1 adduct of $[\gamma\text{-SiW}_{10}\text{O}_{36}]^{8-}$ and $(\text{C}_6\text{H}_6)\text{Ru}^{2+}$, i.e., $\text{Cs}_6[\gamma\text{-SiW}_{10}\text{O}_{36}\text{Ru}(\text{C}_6\text{H}_6)]\cdot 9\text{H}_2\text{O}$, and isolated $[\gamma\text{-SiW}_{10}\text{O}_{36}\text{Ru}(\text{C}_6\text{H}_6)]^{6-}$ is stable in aqueous solution.



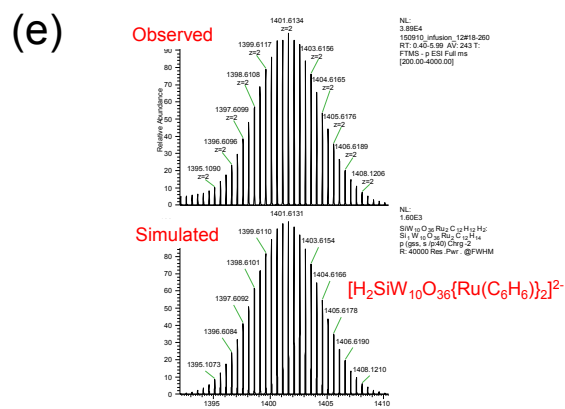


Figure 5. ESI-MS profile. (a), (b), and (c) $[\gamma\text{-SiW}_{10}\text{O}_{36}\text{Ru}(\text{C}_6\text{H}_6)]^{6-}$ dissolved in H_2O /acetonitrile; (b) and (c) are enlarged profiles of (a). (d) and (e) mixture of $\text{K}_8[\gamma\text{-SiW}_{10}\text{O}_{36}]$ and $[\text{Ru}(\text{C}_6\text{H}_6)\text{Cl}_2]_2$ with a $(\text{C}_6\text{H}_6)\text{Ru}^{2+}/[\gamma\text{-SiW}_{10}\text{O}_{36}]^{6-}$ ratio of 2 dissolved in H_2O and then diluted with acetonitrile; (e) is an enlarged profile of (d).

Density Functional Theory Calculations

Eight possible compounds exist for the 1:1 adduct of $[\gamma\text{-SiW}_{10}\text{O}_{36}]^{6-}$ and $(\text{C}_6\text{H}_6)\text{Ru}^{2+}$: two isomers with two of four terminal oxygens on the lacunary site and one water molecule coordinated to $(\text{C}_6\text{H}_6)\text{Ru}^{2+}$ (compounds **1** and **2** in Figure 6), and six isomers with three bridging oxygens of the non-lacunary site coordinated to $(\text{C}_6\text{H}_6)\text{Ru}^{2+}$ (the isolated compound and compounds **3** to **8** in Figure 6). The structure obtained from single-crystal XRD is one of the three most stable compounds from the density functional theory (DFT) calculations; the other two stable isomers are **1** and **3**. These three systems are within 1 kcal/mol of each other based on the DFT calculations. In the Supporting Information, we show the electrostatic potential property of the bare lacunary structure. Figures S1 and S2 explain the preference of the Ru atom for specific oxo sites of the $[\gamma\text{-SiW}_{10}\text{O}_{36}]^{6-}$ surface. In Figure S1, three potential wells are depicted (isosurface value -0.83 a.u.), two of which are equivalent and one large well in the lacuna. These positions correspond to the most nucleophilic sites and, ultimately, to the most stabilizing Ru-POM attaching positions. Figure S2 displays similar information in colored maps, which provide similar results as those reported by Sartorel et al.^[3]

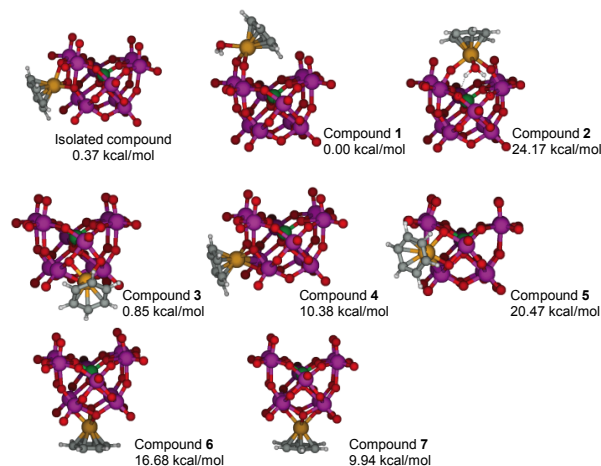


Figure 6. DFT calculations. Eight possible structures obtained for the 1:1 complex of $(\text{C}_6\text{H}_6)\text{Ru}^{2+}$ and $[\gamma\text{-SiW}_{10}\text{O}_{36}]^{6-}$, and their associated relative energies.

We calculated ^{183}W NMR spectra of the three stable compounds (Figure 7) following the procedure described in the Experimental Section. DFT-based NMR calculations of POM compounds are sufficiently accurate for assignments or to quantitatively reproduce observed peaks.^[19] Although the calculated chemical shifts are slightly different from the observed values, the peaks for the tungsten atoms that are close to Ru in the isolated compound —W(7,8) and W(9,10)— are downfield-shifted, as in the spectrum shown in Figure 4. For compound **1**, no clear downfield shift is observed. For compound **3**, six singlets should be observed. These results also support that the structure observed by single-crystal XRD is stable in aqueous solution.

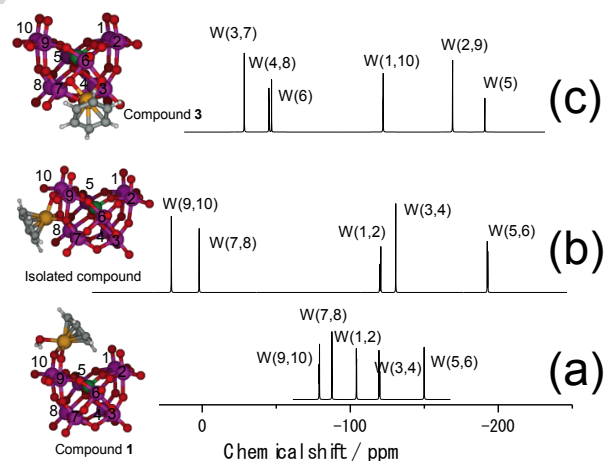


Figure 7. Calculated ^{183}W NMR chemical shifts of (a) compound **1**, (b) the isolated compound, and (c) compound **3**.

Acid-Base Titration

A titration curve was obtained by adding 1.0 M NaOH to a 0.1 M NaClO_4 and 0.01 M HClO_4 (pH 2.0) solution containing 1 mM

$K_8[\gamma\text{-SiW}_{10}\text{O}_{36}]$ or $\text{Cs}_6[\gamma\text{-SiW}_{10}\text{O}_{36}\text{Ru}(\text{C}_6\text{H}_6)]$ (Figure 8). The initial pH value slightly increases to 2.2 when 1 mM $K_8[\gamma\text{-SiW}_{10}\text{O}_{36}]$ is dissolved, and the pH begins to increase when NaOH is added to a concentration of 9 mM; the slope of the pH increase becomes slightly less steep when the NaOH concentration increases to ~9–10 mM. Then, the pH value becomes constant at ~7.3 when the NaOH concentration surpasses 10 mM. The dissolved $[\gamma\text{-SiW}_{10}\text{O}_{36}]^{8-}$ receives one proton (Equation 1), and the pH of the solution increases ($-\log 0.009 = 2.1$). The pK_a of this proton is ~6.7 (Equation 2); therefore, the slope of the pH increase becomes gentle between pH values of 6.0 and 7.3. Deprotonated $[\gamma\text{-SiW}_{10}\text{O}_{36}]^{8-}$ starts to decompose at $\text{pH} \approx 7.3$, which is close to the reported decomposition pH value of 8.^[14]



In contrast, the initial pH value does not change for $\text{Cs}_6[\gamma\text{-SiW}_{10}\text{O}_{36}\text{Ru}(\text{C}_6\text{H}_6)]$; the pH value starts to increase when the NaOH concentration reaches ~10 mM and it becomes constant at a pH of ~7.7, indicating that $[\gamma\text{-SiW}_{10}\text{O}_{36}\text{Ru}(\text{C}_6\text{H}_6)]^{6-}$ is not protonated and $[\gamma\text{-SiW}_{10}\text{O}_{36}\text{Ru}(\text{C}_6\text{H}_6)]^{6-}$ starts to decompose at pH of ~7.7.

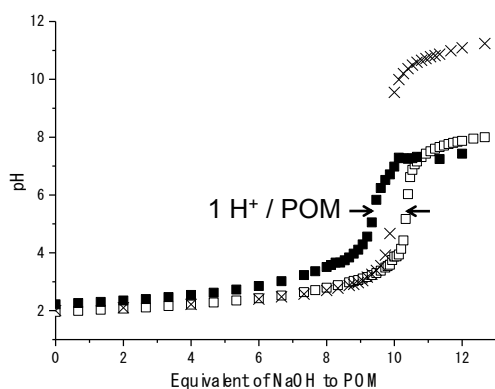


Figure 8. pH titration curves of (x) blank (the NaOH solution was added to 0.1 M of NaClO_4 containing 0.01 M HClO_4 (pH 2.0)), (closed square) in the presence of 1.0 mM of $K_8[\gamma\text{-SiW}_{10}\text{O}_{36}]$, and (open square) 1.0 mM of $\text{Cs}_6[\gamma\text{-SiW}_{10}\text{O}_{36}\text{Ru}(\text{C}_6\text{H}_6)]$.

Cyclic Voltammetry

$[\gamma\text{-SiW}_{10}\text{O}_{36}]^{8-}$ shows redox couples at -713 and -818 mV in an acetate buffer (1 M acetic acid + 1 M sodium acetate, pH 4.7); these values are similar to those reported for two-electron redox of W (-750 and -840 mV vs. saturated calomel electrode) (Figure 9).^[14] The cyclic voltammogram (CV) of $[\gamma\text{-SiW}_{10}\text{O}_{36}\text{Ru}(\text{C}_6\text{H}_6)]^{6-}$ in the same acetate buffer shows a reversible redox couple at -698 mV and an irreversible oxidation peak at ~1320 mV. The stability of $[\gamma\text{-SiW}_{10}\text{O}_{36}\text{Ru}(\text{C}_6\text{H}_6)]^{6-}$ in the acetate buffer is confirmed by ^1H NMR, showing a singlet at 5.93 ppm (Figure 3b). The peak currents of these redox reactions are linearly dependent on the square of the scan rates, indicating that the redox reactions are

diffusion-controlled. The reversible redox couple is assignable to the two-electron redox couple on W, and the oxidation peak is assignable to oxidation of Ru. The oxidation potential of Ru is higher than that of the other Ru-containing silicotungstates, such as mono-Ru substituted silicotungstate derivatives ($[\text{SiW}_{11}\text{O}_{39}\text{Ru}(\text{L})]^{7-}$, $\text{L} = \text{H}_2\text{O}$, CO , pyridine, DMSO)^[17, 20] and a tetra-Ru-containing sandwiched compound, $[(\gamma\text{-SiW}_{10}\text{O}_{36})_2\{\text{Ru}_4\text{O}_4(\text{OH})_4(\text{H}_2\text{O})_4\}]^{10-}$.^[21]

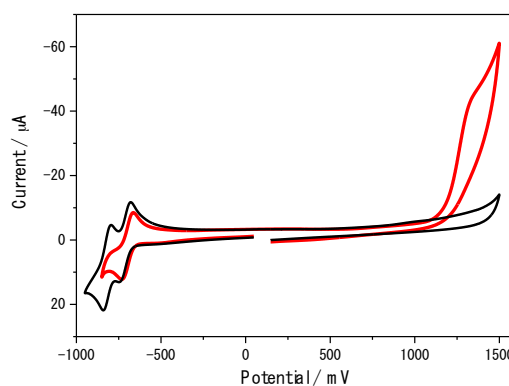


Figure 9. Cyclic voltammograms of (black line) $K_8[\gamma\text{-SiW}_{10}\text{O}_{36}]$ (1 mM) and (red line) $\text{Cs}_6[\gamma\text{-SiW}_{10}\text{O}_{36}\text{Ru}(\text{C}_6\text{H}_6)]$ (1 mM) dissolved in acetate buffer (pH 4.7).

UV-Vis

UV-Vis spectra are compared for $K_8[\gamma\text{-SiW}_{10}\text{O}_{36}]$ and $\text{Cs}_6[\gamma\text{-SiW}_{10}\text{O}_{36}\text{Ru}(\text{C}_6\text{H}_6)]$ in the acetate buffer (Figure S3). $[\gamma\text{-SiW}_{10}\text{O}_{36}\text{Ru}(\text{C}_6\text{H}_6)]^{6-}$ also absorbs visible light, while $K_8[\gamma\text{-SiW}_{10}\text{O}_{36}]$ only absorbs UV light.

Monitoring the $[\gamma\text{-SiW}_{10}\text{O}_{36}]^{8-}$ and $[\text{Ru}(\text{C}_6\text{H}_6)\text{Cl}_2]_2$ Reaction Mixture

The reactivity of $(\text{C}_6\text{H}_6)\text{Ru}^{2+}$ on $[\gamma\text{-SiW}_{10}\text{O}_{36}]^{8-}$ was monitored using ^1H NMR for mixtures of $[\gamma\text{-SiW}_{10}\text{O}_{36}]^{8-}$ and $[\text{Ru}(\text{C}_6\text{H}_6)\text{Cl}_2]_2$ with different $(\text{C}_6\text{H}_6)\text{Ru}^{2+}/[\gamma\text{-SiW}_{10}\text{O}_{36}]^{8-}$ ratios in D_2O (Figure 10). The ^1H NMR spectrum of $[\text{Ru}(\text{C}_6\text{H}_6)\text{Cl}_2]_2$ shows several singlets because $[\text{Ru}(\text{C}_6\text{H}_6)\text{Cl}_2]_2$ forms several isomers in water (Figure 4 (a)).^[22] When the $(\text{C}_6\text{H}_6)\text{Ru}^{2+}/[\gamma\text{-SiW}_{10}\text{O}_{36}]^{8-}$ ratio is less than 1.0, a new product is produced, showing a singlet at 5.98 ppm (Figure 10b, c), which is the same as the ^1H NMR spectrum of isolated $[\gamma\text{-SiW}_{10}\text{O}_{36}\text{Ru}(\text{C}_6\text{H}_6)]^{6-}$, indicating that $[\gamma\text{-SiW}_{10}\text{O}_{36}\text{Ru}(\text{C}_6\text{H}_6)]^{6-}$ forms immediately. Further addition of $[\text{Ru}(\text{C}_6\text{H}_6)\text{Cl}_2]_2$ produces the other product, showing four singlets at 5.89, 5.90, 5.92, and 6.01 ppm (Figure 10d-g, black arrows). The four singlets are the same as the ^1H NMR singlets of the di- $\text{Ru}(\text{C}_6\text{H}_6)$ -containing $[\gamma\text{-SiW}_{10}\text{O}_{36}]^{8-}$ compound, $[\gamma\text{-SiW}_{10}\text{O}_{36}\text{Ru}(\text{C}_6\text{H}_6)\{\text{Ru}(\text{C}_6\text{H}_6)(\text{H}_2\text{O})\}]^{4-}$, reported by Kortz and Nadjo.^[11] A clear explanation for why the di- $\text{Ru}(\text{C}_6\text{H}_6)$ -containing $[\gamma\text{-SiW}_{10}\text{O}_{36}]^{8-}$ shows four singlets was presented in their paper. The presence of four singlets indicates that there are four different $\text{Ru}(\text{C}_6\text{H}_6)$ functional groups in the solution. The ESI mass spectrum of the solution with a 2:1 mixture of $\text{Ru}(\text{C}_6\text{H}_6)^{2+}$ and $[\gamma\text{-SiW}_{10}\text{O}_{36}]^{8-}$ shows peaks of the 1:1 product, $[\gamma\text{-SiW}_{10}\text{O}_{36}\text{Ru}(\text{C}_6\text{H}_6)]^{6-}$, and the 2:1 product $[\gamma\text{-}$

$\text{SiW}_{10}\text{O}_{36}\{\text{Ru}(\text{C}_6\text{H}_6)\}_2\}^{4-}$ (Figures 5d and e). The four singlets of the solution with a $(\text{C}_6\text{H}_6)\text{Ru}^{2+}/[\gamma\text{-SiW}_{10}\text{O}_{36}]^{8-}$ ratio of 2 disappear by the addition of $[\gamma\text{-SiW}_{10}\text{O}_{36}]^{8-}$, while the singlet at 5.98 ppm remains. These results indicate that the 2:1 product, $[\gamma\text{-SiW}_{10}\text{O}_{36}\{\text{Ru}(\text{C}_6\text{H}_6)\}_2]^{4-}$, is present in the solution.

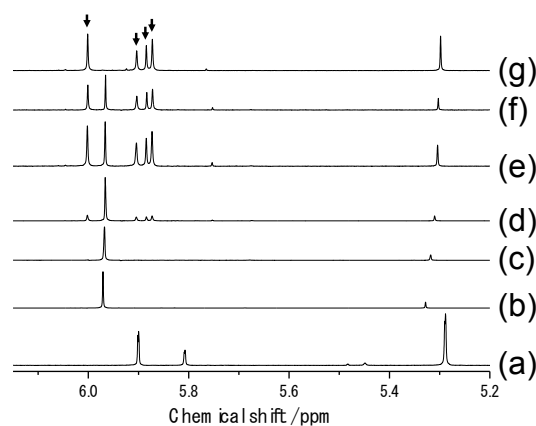


Figure 10. ^1H NMR of a D_2O solution containing $[\text{Ru}(\text{C}_6\text{H}_6)\text{Cl}_2]_2$ and $[\gamma\text{-SiW}_{10}\text{O}_{36}]^{8-}$ with different $(\text{C}_6\text{H}_6)\text{Ru}^{2+}/[\gamma\text{-SiW}_{10}\text{O}_{36}]^{8-}$ ratios of (a) 1:0, (b) 1:0.5, (c) 1:1, (d) 1:1.5, (e) 1:2, (f) 1:3, (g) 1:4. The arrows indicate peaks assignable to $[\gamma\text{-SiW}_{10}\text{O}_{36}\text{Ru}(\text{C}_6\text{H}_6)\{\text{Ru}(\text{C}_6\text{H}_6)(\text{H}_2\text{O})\}]^{4-}$, as reported by the Kortz and Nadjjo group.^[11]

The diffusion ordered spectroscopy (DOSY) ^1H NMR spectra of the mixtures of $[\gamma\text{-SiW}_{10}\text{O}_{36}]^{8-}$ and $[\text{Ru}(\text{C}_6\text{H}_6)\text{Cl}_2]_2$ with a $(\text{C}_6\text{H}_6)\text{Ru}^{2+}/[\gamma\text{-SiW}_{10}\text{O}_{36}]^{8-}$ ratio of 2 indicate that the species showing four singlets have different diffusion coefficients than the 1:1 species, $[\gamma\text{-SiW}_{10}\text{O}_{36}\text{Ru}(\text{C}_6\text{H}_6)]^{6-}$ (Figure 11). The diffusion coefficient of the species showing singlets at 5.89 ppm is larger than that of $[\gamma\text{-SiW}_{10}\text{O}_{36}\text{Ru}(\text{C}_6\text{H}_6)]^{6-}$. However, the diffusion coefficients of species showing singlets at 5.90, 5.92, and 6.01 ppm are smaller than that for $[\gamma\text{-SiW}_{10}\text{O}_{36}\text{Ru}(\text{C}_6\text{H}_6)]^{6-}$. We propose that isomers of di- $\text{Ru}(\text{C}_6\text{H}_6)$ -containing $[\gamma\text{-SiW}_{10}\text{O}_{36}]^{8-}$ exist in water, whereby the binding position of $(\text{C}_6\text{H}_6)\text{Ru}^{2+}$ is different, and the $[\gamma\text{-SiW}_{10}\text{O}_{36}\text{Ru}(\text{C}_6\text{H}_6)\{\text{Ru}(\text{C}_6\text{H}_6)(\text{H}_2\text{O})\}]^{4-}$ compound isolated by Kortz and Nadjjo^[11] is one of the isomers. These results indicate that $(\text{C}_6\text{H}_6)\text{Ru}^{2+}$ reacts with $[\gamma\text{-SiW}_{10}\text{O}_{36}]^{8-}$ first to form the 1:1 compound; further addition of $(\text{C}_6\text{H}_6)\text{Ru}^{2+}$ produces the 2:1 compound (Figure 12).

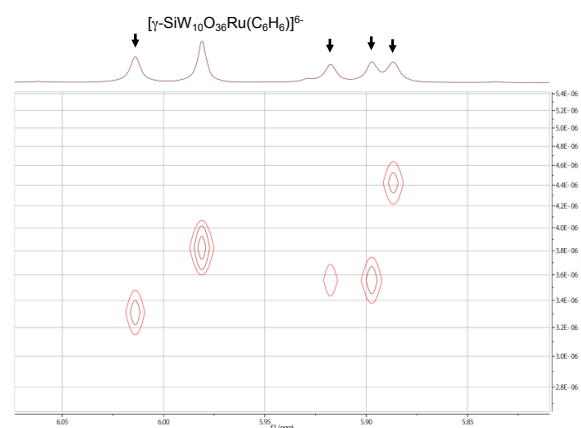


Figure 11. DOSY ^1H NMR spectrum of a D_2O solution containing $[\text{Ru}(\text{C}_6\text{H}_6)\text{Cl}_2]_2$ and $[\gamma\text{-SiW}_{10}\text{O}_{36}]^{8-}$ with a $(\text{C}_6\text{H}_6)\text{Ru}^{2+}/[\gamma\text{-SiW}_{10}\text{O}_{36}]^{8-}$ ratio of 2:1.

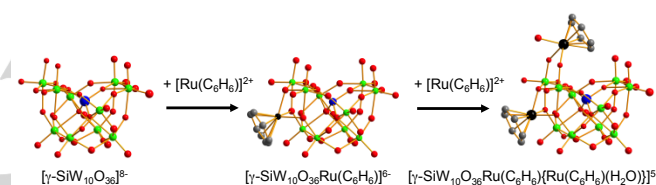


Figure 12. Schematic presentation of the reaction of $(\text{C}_6\text{H}_6)\text{Ru}^{2+}$ with $[\gamma\text{-SiW}_{10}\text{O}_{36}]^{8-}$.

Conclusions

A 1:1 complex of $(\text{benzene})\text{Ru}^{2+}$ and di-lacunary gamma-type silicotungstate, $[\gamma\text{-SiW}_{10}\text{O}_{36}\text{Ru}(\text{C}_6\text{H}_6)]^{6-}$, was isolated as a cesium salt by reaction of $\text{K}_8[\gamma\text{-SiW}_{10}\text{O}_{36}]$ and $[\text{Ru}(\text{C}_6\text{H}_6)\text{Cl}_2]_2$ with a $(\text{C}_6\text{H}_6)\text{Ru}^{2+}/[\gamma\text{-SiW}_{10}\text{O}_{36}]^{8-}$ ratio of 1. Characterization by single-crystal X-ray structure analysis; ^1H , ^{13}C , and ^{183}W NMR spectroscopy; ^{13}C MAS NMR spectroscopy; IR spectroscopy; elemental analysis; and high-resolution ESI mass spectrometry (MS) clearly demonstrated that the single $(\text{C}_6\text{H}_6)\text{Ru}^{2+}$ moiety was attached on three bridging oxygens of the non-lacunary site. The relative stability of isomers and ^{183}W NMR assignments for the most stable ones, computed at the density functional level, support the conclusions derived from experiments. We revealed that $(\text{C}_6\text{H}_6)\text{Ru}^{2+}$ first reacted on the bridging oxygens of the non-lacunary site to form $[\gamma\text{-SiW}_{10}\text{O}_{36}\text{Ru}(\text{C}_6\text{H}_6)]^{6-}$, and then reacted on the terminal oxygens of the lacunary site to form a 2:1 $[\gamma\text{-SiW}_{10}\text{O}_{36}\text{Ru}(\text{C}_6\text{H}_6)\{\text{Ru}(\text{C}_6\text{H}_6)(\text{H}_2\text{O})\}]^{4-}$ complex, which existed as an isomeric mixture in water.

Experimental Section

Materials: Deionized water (Millipore, Elix) was used for all experiments. $\text{K}_8[\gamma\text{-SiW}_{10}\text{O}_{36}]\cdot 6.9\text{H}_2\text{O}$ was prepared according to a published procedure and analyzed by IR, cyclic voltammetry, and thermogravimetry-

differential thermal analysis.^[14] All other chemicals were commercial reagents and used as supplied.

Preparation of Cs₆[γ-SiW₁₀O₃₆Ru(C₆H₆)]·9H₂O: K₈[γ-SiW₁₀O₃₆]-6.9H₂O (0.357 g, 0.124 mmol) and [Ru(C₆H₆)Cl₂]₂ (0.031 g, 0.062 mmol) were dissolved in water (15 mL) and stirred at room temperature for 1 h. The orange solution was filtered and CsCl (1.5 g) was added to the filtrate; the solution was stirred at room temperature for 1 h, and the solution was stored in a refrigerator for 24 h. The produced orange solid was removed by filtration (~0.18 g). The orange solid (~0.1 g) was then dissolved in 3.5 mL of water at room temperature for 1 h, and the solution was centrifuged (3000 rpm for 6 min; H-27F, Kokusan) to remove the non-dissolved solid. The vessel containing the clear orange solution was placed in a closed beaker with room-temperature ethanol to obtain orange crystals. The produced orange crystal was filtered and dried at 70 °C (0.071 g, 16.1% based on W).

IR (KBr): (ν/cm⁻¹) = 985.9 (w), 943.1 (m), 908.7 (s), 869.4 (vs), 750.6 (s). ¹H NMR (D₂O): (δ/ppm) 5.99. ¹³C NMR (D₂O): (δ/ppm) 81.61. ¹⁸³W NMR (D₂O): (δ/ppm) -25.88, -50.06, -140.10, -150.85, and -187.17. Elemental analysis: calculated for Cs₆[SiW₁₀O₃₆Ru(C₆H₆)]·0.1KCl·8H₂O: (%) H 0.50; Si 0.87; C 2.02; W 51.49; Ru 2.83; Cs 22.3; K 0.1; Cl 0.1, found: (%) H 0.66; Si 0.83; C 2.15; W 51.44; Ru 2.8; Cs 22.2; K 0.1; Cl 0.1. Negative

Table 1. Crystal data and structural refinement of a cesium salt of Cs₆[SiW₁₀O₃₆Ru(C₆H₆)].

Empirical formula	Cs ₆ [SiW ₁₀ O ₃₆ Ru(C ₆ H ₆)]·9H ₂ O
Molecular weight/g·mol ⁻¹	3446.01
Crystal color and shape	Orange, prism
Temperature/K	123
Crystal system	Monoclinic
Space group (no.)	P 2 ₁ m (no. 14)
a/Å	9.697(13)
b/Å	12.295(17)
c/Å	43.38(6)
β/°	91.843(19)
Volume/Å ³	5169(12)
Z	4
Data/parameters	11662/595
R(int)	0.1424
Density (calcd)/gcm ⁻³	4.428
Abs. coefficient/mm ⁻¹	26.463
R ₁ (I > 2 s(I)) ^[a]	0.0978
wR ₂ (all data) ^[b]	0.2349

[a] $R_1 = \sum ||F_o| - |F_c|| / \sum |F_o|$, [b] $R_w = [\sum w(F_o^2 - F_c^2)^2] / \sum [w(F_o^2)^2]^{1/2}$.

ion MS (CH₃CN-H₂O): calculated for [H₂SiW₁₀O₃₅Ru(C₆H₆)]²⁻ m/z = 1303.6391, found m/z = 1303.6387.

X-ray crystallography: Single-crystal XRD data of a crystal (0.170×0.150×0.100 mm) were collected using a Rigaku Saturn724 diffractometer at -163 °C using multi-layer mirror monochromated Mo-K_α radiation (λ = 0.71075 Å). Data were collected and processed using the CrystalClear software (Rigaku Co. Tokyo). An empirical absorption correction was applied, providing transmission factors from 0.051 to 0.071. The data were corrected for Lorentz and polarization effects. The structure was solved using the direct method^[23] and expanded using Fourier techniques. All atoms (W, Ru, P, O, K) except for carbon were refined anisotropically. Calculations were performed using the CrystalStructure 4.1 crystallographic software package (Rigaku Co. Tokyo) except for refinement, which was performed using SHELX-97.^[24] The data set was corrected using the SQUEEZE program,^[25] which is part of the PLATON package of crystallographic software used to calculate the solvent or counterion disorder area and to remove its contribution to the overall intensity data; some water molecules and cesium atoms were omitted by the PLATON SQUEEZE procedure. Therefore, the number of cesium atoms and water oxygen atoms determined by XRD is smaller than that determined by elemental analysis. The crystallographic data are summarized in Table 1. Further details of the crystal structure can be obtained from the Cambridge Crystallographic Data Centre (CCDC), 12 Union Road, Cambridge CB2 1EZ, UK [fax.: +44 1223/336-033; E-mail: deposit@ccdc.cam.ac.uk], upon quoting depository number CCDC 1581623.

Other analytical techniques: IR spectra were recorded using a Nicolet 6700 FT-IR spectrometer (Thermo Fisher Scientific) using KBr pellets. Cyclic voltammetry was performed on a CHI620D system (BAS Inc.) at ambient temperature. A glassy carbon working electrode (diameter = 3 mm), platinum wire counter electrode, and Ag/AgCl reference electrode (203 mV vs. normal hydrogen electrode (NHE) at 25 °C) (3 M NaCl, BAS Inc.) were used. Approximate formal potential values (E_{1/2} values) were calculated from the CVs as the average of the cathodic and anodic peak potentials for the corresponding oxidation and reduction waves. UV-Vis spectra were recorded at ambient temperature using an 8453 UV-Vis spectrometer (Agilent) with a 1-cm quartz cell. ¹H and ¹³C NMR spectra were recorded on a Varian 500 spectrometer (500 MHz, Agilent) (H and C resonance frequencies: 499.939 and 125.723 MHz, respectively). The spectra were referenced to internal HOD (4.659 ppm) or acetone (30.14 and 21.534 ppm) for ¹H or ¹³C NMR, respectively. DOSY NMR experiments were carried out at 25 °C without sample spinning using the same NMR spectrometer. Solid-state ¹³C MAS NMR spectra were recorded at 150.87 MHz on a Varian 600PS solid NMR spectrometer using a 3.2-mm-diameter zirconia rotor at 20 kHz. ¹H-¹³C dipolar decoupling MAS NMR spectra were obtained at a 180° pulse length of 2.35 μs, cycle delay time of 50 s, and 128 scans. ¹³C chemical shifts were referenced to hexamethylbenzene. Elemental analyses were carried out by Mikroanalytisches Labor Pascher (Remagen, Germany). High-resolution ESI-MS was performed using an LTQ Orbitrap XL spectrometer (Thermo Fisher Scientific) with an accuracy of 3 ppm. Each sample (5 mg) was dissolved in 5 mL of H₂O, and the solutions were diluted with CH₃CN (final concentration: ~10 μg/mL).

Density functional calculations(DFT): DFT calculations were performed using the ADF 2016 program package.^[26] Different basis sets and density functionals of the generalized gradient approximation (GGA) type were used at different stages of the computational procedure, as outlined below. First, we performed full geometry optimizations on eight

isomeric forms, including $[\gamma\text{-SiW}_{10}\text{O}_{36}\text{Ru}(\text{C}_6\text{H}_6)]^{6-}$ and $[\gamma\text{-SiW}_{10}\text{O}_{36}\text{Ru}(\text{C}_6\text{H}_6)(\text{H}_2\text{O})]^{5-}$. When possible, we exploited the C_s point group symmetry to save computational time. We applied the BP86 functional and basis sets of triple- ζ + double polarization (TZ2P) quality with the (medium-sized) frozen core approximation, together with scalar relativistic effects using the zeroth-order regular approximation. We added the effects of an aqueous solution using the conductor-like screening model (COSMO)^[27] characterized by dielectric constant, $\epsilon = 78.4$. Second, we carried out the NMR study for the three lowest-energy systems. Inspired by the work of Vilà-Nadal et al. for ^{183}W NMR calculations on POMs,^[19c] the selected structures were re-optimized with all-electron QZ4P (quadruple zeta with four polarization functions) basis sets and the Perdew-Burke-Ernzerhof (PBE) functional including solvent effects with the COSMO and high numerical accuracy. These calculations were followed by all-electron OPBE/TZ2P/COSMO single-point calculations while considering relativistic spin-orbit effects (OPBE combines the PBE functional with Handy's optimized exchange). In addition to the latter electron density, we calculated the shielding ^{183}W NMR parameters as implemented in the ADF 2016 program package. The computed chemical shifts presented are referred to that of the reference compound $[\text{WO}_4]^{2-}$ in aqueous solution.

Acknowledgements

This research was supported by JSPS KAKENHI grant number JP26420787 (Grand-in-Aid for Scientific Research Scientific (C)) and the Center for Functional Nano Oxide at Hiroshima University. X. L. thanks national project CTQ2014-52774-P from the Ministry of Economy, Industry and Competitiveness of Spain. We thank Ms. T. Amimoto and Ms. N. Kawata at the Natural Science Center for Basic Research and Development (N-BARD), Hiroshima University for the ESI-MS measurement and initial single-crystal X-ray structure analysis, respectively.

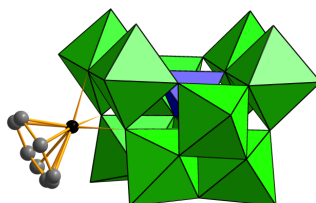
Keywords: Polyoxometalates • γ -Keggin silicotungstate • Ruthenium • Isomers

- [1] a) C. L. Hill, *Special Thematic Issue on Polyoxometalates*, *Chem. Rev.* **1998**, *98*, 1-390; b) M. T. Pope, *Heteropoly and Isopoly Oxometalates*, Springer-Verlag, Berlin, **1983**; c) L. Cronin, *Special Thematic Issue on Polyoxometalates*, *Chem. Soc. Rev.* **2012**, *41*, 7325-7648.
- [2] a) K. Kamata, *Bull. Chem. Soc. Jpn.* **2015**, *88*, 1017-1028; b) K. Kamata, K. Yonehara, Y. Sumida, K. Yamaguchi, S. Hikichi, N. Mizuno, *Science* **2003**, *300*, 964-966; c) N. Mizuno, K. Kamata, K. Yamaguchi, *Top. Catal.* **2011**, *53*, 876-893; d) N. Mizuno, K. Yamaguchi, K. Kamata, *Catal. Surv. Asia*, **2011**, *15*, 68-79.
- [3] A. Sartorel, M. Carraro, A. Bagno, G. Scorrano, M. Bonchio, *Angew. Chem. Int. Ed.* **2007**, *46*, 3255-3258.
- [4] K. Suzuki, J. Jeong, K. Yamaguchi, N. Mizuno, *Chem. Asian-J.* **2016**, *10*, 144-148.
- [5] K. Sugahara, S. Kuzuya, T. Hirano, K. Kamata, N. Mizuno, *Inorg. Chem.* **2012**, *51*, 7932-7939.
- [6] a) N. Mizuno, K. Kamata, *Coord. Chem. Rev.* **2011**, *255*, 2358-2370; b) K. Suzuki, F. Tang, Y. Kikukawa, K. Yamaguchi, N. Mizuno, *Angew. Chem. Int. Ed.* **2014**, *53*, 5356-5360.
- [7] R. Sato, K. Suzuki, M. Sugawa, N. Mizuno, *Chem. Euro.-J.* **2013**, *19*, 12982-12990.
- [8] H. Lv, Y. V. Geletii, C. Zhao, J. W. Vickers, G. Zhu, Z. Luo, J. Song, T. Lian, D. G. Musaev, C. L. Hill, *Chem. Soc. Rev.* **2012**, *41*, 7572-7589.
- [9] a) N. V. Izarova, M. T. Pope, U. Kortz, *Angew. Chem. Int. Ed.* **2012**, *51*, 9492-9510; b) P. Putaj, F. Lefebvre, *Coord. Chem. Rev.* **2011**, *255*, 1642-1685.
- [10] P. A. Abramov, T. P. Zemerova, M. N. Sokolov, *J. Clust. Sci.* **2017**, *28*, 725-734.
- [11] L.-H. Bi, E. V. Chubarova, N. H. Nsouli, M. H. Dickman, U. Kortz, B. Keita, L. Nadjo, *Inorg. Chem.* **2006**, *45*, 8575-8583.
- [12] L.-H. Bi, U. Kortz, M. H. Dickman, B. Keita, L. Nadjo, *Inorg. Chem.* **2005**, *44*, 7485-7493.
- [13] a) M. Bonchio, G. Scorrano, P. Toniolo, A. Proust, V. Artero, V. Conte, *Adv. Synth. Catal.* **2002**, *344*, 841-844; b) C. Kato, A. Shinohara, N. Moriya, K. Nomiyama, *Catal. Commun.* **2006**, *7*, 413-416; c) R.-Q. Meng, L. Suo, G.-F. Hou, J. Liang, L.-H. Bi, H.-L. Li, L.-X. Wu, *CrystEngComm* **2013**, *15*, 5867-5876; d) R.-Q. Meng, B. Wang, H.-M. Sui, B. Li, W. Song, L.-X. Wu, B. Zhao, L.-H. Bi, *Eur. J. Inorg. Chem.* **2013**, 1935-1942; e) D.-M. Zheng, R.-Q. Wang, D. Y., G.-F. Hou, L.-X. Wu, L.-H. Bi, *New J. Chem.* **2016**, *40*, 8829-8836; f) L.-H. Bi, G. Al-Kadamany, E. V. Chubarova, M. H. Dickman, L. Chen, D. S. Gopala, R. M. Richards, B. Keita, L. Nadjo, H. Jaensch, G. Mathys, U. Kortz, *Inorg. Chem.* **2009**, *48*, 10068-10077.
- [14] A. Tézé, G. Hervé, *Inorg. Synth.* **1990**, *27*, 85-96.
- [15] C. Rong, M. T. Pope, *J. Am. Chem. Soc.* **1992**, *114*, 2932-2938.
- [16] M. Sadakane, N. Rinn, S. Moroi, H. Kitatomi, T. Ozeki, M. Kurasawa, M. Itakura, S. Hayakawa, K. Kato, M. Miyamoto, S. Ogo, Y. Ide, T. Sano, *Z. Anorg. Allgem. Chem.* **2011**, *637*, 1467-1474.
- [17] M. Sadakane, Y. Iimuro, D. Tsukuma, B. S. Bassil, M. H. Dickman, U. Kortz, Y. Zhang, S. Ye, W. Ueda, *Dalton Trans.* **2008**, 6692-6698.
- [18] a) V. Artero, V. Lahootun, R. Villanneau, R. Thouvenot, P. Herson, P. Gouzerh, A. Proust, *Inorg. Chem.* **2005**, *44*, 2826-2835; b) D. Laurencin, R. Villanneau, P. Herson, R. Thouvenot, Y. Jeannin, A. Proust, *Chem. Commun.* **2005**, 5524-5526.
- [19] a) J. Gracia, J. M. Poblet, J. A. Fernández, J. Autschbach, L. P. Kazansky, *Eur. J. Inorg. Chem.* **2006**, 1149-1154; b) J. Gracia, J. M. Poblet, J. Autschbach, L. P. Kazansky, *Eur. J. Inorg. Chem.* **2006**, 1139-1148; c) L. Vilà-Nadal, J. P. Sarasa, A. Rodríguez-Fortea, J. Igual, L. P. Kazansky, J. M. Poblet, *Chem. Asian-J.* **2010**, *5*, 97-104; d) M. Pascual-Borrás, X. López, A. Rodríguez-Fortea, R. J. Errington, J. M. Poblet, *Chem. Sci.* **2014**, *5*, 2031-2042.
- [20] a) M. Sadakane, S. Moroi, Y. Iimuro, N. Izarova, U. Kortz, S. Hayakawa, K. Kato, S. Ogo, Y. Ide, W. Ueda, T. Sano, *Chem. Asia. J.* **2012**, *7*, 1331-1339; b) K. Nishiki, N. Umehara, Y. Kadota, X. López, J. M. Poblet, C. A. Mezui, A.-L. Teillout, I. M. Mbomekalle, P. de Oliveira, M. Miyamoto, T. Sano, M. Sadakane, *Dalton Trans.* **2016**, *45*, 3715-3726; c) S. Ogo, N. Shimizu, K. Nishiki, N. Yasuda, T. Mizuta, T. Sano, M. Sadakane, *Inorg. Chem.* **2014**, *53*, 3526-3539.
- [21] Y. Liu, S.-X. Guo, A. M. Bond, J. Zhang, Y. V. Geletii, C. L. Hill, *Inorg. Chem.* **2013**, *52*, 11986-11996.
- [22] a) R. A. Zelonka, M. C. Baird, *Can. J. Chem.* **1972**, *50*, 3063-3072; b) R. O. Gould, C. L. Jones, D. R. Robertson, T. A. Stephenson, *J. Chem. Soc., Chem. Commun.* **1977**, 222-223; c) M. A. Bennett, A. K. Smith, *J. Chem. Soc., Dalton Trans.* **1974**, 233-2241.
- [23] L. Palatinus, G. Chapuis, *J. Appl. Crystallogr.* **2007**, *40*, 786-790.
- [24] G. M. Sheldrick, *Acta Crystallogr., Sect. A* **2008**, *64*, 112-122.
- [25] P. van der Sluis, A. L. Spek, *Acta Crystallogr., Sect. A* **1990**, *46*, 194-201.
- [26] a) C. Fonseca Guerra, J. G. Snijders, G. Te Velde, E. J. Baerends, *Theor. Chem. Acc.* **1998**, *99*, 391-403; b) G. Te Velde, F. M. Bickelhaupt, S. J. A. van Gisbergen, C. Fonseca Guerra, E. J. Baerends, J. G. Snijders, T. Ziegler, *J. Comput. Chem.* **2001**, *22*, 931-967.
- [27] a) A. Klamt, *J. Phys. Chem.* **1995**, *99*, 2224-2235; b) J. Andzelm, C. Kölmel, A. Klamt, *J. Chem. Phys.* **1995**, *103*, 9312-9320; c) A. Klamt, G. Schürmann, *J. Chem. Soc. Perkin Trans.* **1993**, *2*, 799-805; d) C. C. Pye, T. Ziegler, *Theor. Chem. Acc.* **1999**, *101*, 396-408.

Entry for the Table of Contents

FULL PAPER

A reaction of a (benzene)Ru²⁺ complex with a di-lacunary γ -Keggin-type silicodecatungstate, K₈[γ -SiW₁₀O₃₆] with a (C₆H₆)Ru²⁺/[γ -SiW₁₀O₃₆]⁸⁻ ratio of 1 produces [γ -SiW₁₀O₃₆Ru(C₆H₆)]⁶⁻.

**Ru- γ -Keggin di-lacunary silicotungstate**

*Masaya Kikuchi, Hiromi Ota, Xavier López, Toshimi Nakaya, Nao Tsunoji, Tsuneji Sano, Masahiro Sadakane**

Page No. – Page No.

Reactivity of a (Benzene)Ruthenium(II) Cation on Di-lacunary γ -Keggin-Type Silicotungstate and Synthesis of a Mono-(Benzene)Ruthenium(II)-Attached γ -Keggin-Type Silicotungstate